Nitrogen immobilization caused by chemical formation of black- and amide-N in soil

Jing Wei[a,b,e*], Heike Knicker[c], Zheyan Zhou[a], Kai-Uwe Eckhardt[f], Peter Leinweber[f], Holger Wissel[b], Wenping Yuan[a,d,e], Nicolas Brüggemann[b]

[a]*School of Atmospheric Sciences, Sun Yat-sen University, Zhuhai, Guangdong, 519082, China*

[b]*Forschungszentrum Jülich GmbH, Institute of Bio- and Geosciences, Agrosphere (IBG-3), Wilhelm-Johnen-Straße, 52425 Jülich, Germany*

[c]*Instituto de Recursos Naturales y Agrobiología, CSIC, P.O. Box 1052, E-41080 Sevilla, Spain*

[d]*Guangdong Province Key Laboratory for Climate Change and Natural Disaster Studies, Sun Yat-sen University, Zhuhai 519082, China*

[e]*Southern Marine Science and Engineering Guangdong Laboratory (Zhuhai), Zhuhai, Guangdong, 519082, China*

[f]*Soil Science, University of Rostock, Justus-von-Liebig-Weg 6, Rostock, 18051 Germany*

**Corresponding author:*

Current address: Email, weiji53@mail.sysu.edu.cn; Tel, +86 756 3668557; Fax, +86 756 3668569

Abstract

Nitrogen (N) immobilization controls the N availability in soil, however, mechanisms involved in the chemical N fixation into soil organic N (SON) through reactions of reactive N compounds with soil organic matter (SOM) is not clear. Knowledge about the composition and stability of chemically produced SON is limited, which impedes understanding of the interplay of N and carbon (C) cycles at both the local and global scale. Here, we studied the chemical N immobilization of nitrite in soils from grassland, cropland, and forest with ^{15}N labelling technique. And solid state ^{15}N- and ^{13}C-NMR spectroscopies were applied to further explore the structure of chemically immobilized SON. We found that the chemical retention rate of nitrite did not differ significantly between land-uses, while the fulvic acid fraction was the SOM component most reactive to nitrite. In contrast to the common assumption that amides are mainly of biological origin and that black N compounds are formed from organic N compounds at high temperature during fires, our study revealed that amides and black N in the form of pyrroles were the main products of chemical reactions of nitrite with SOM. These findings indicate that chemical processes play a key role in biogeochemical N cycling, and provide new insight into the mechanisms of C–N interactions in soil.

Keywords: chemical nitrogen immobilization, nitrite, soil organic matter, amide, black nitrogen

1. Introduction

Nitrogen (N) is an essential element for living organisms and a growth-limiting nutrient of agricultural crops. To promote food production, industrial N fertilizers have been widely used since the Haber-Bosch process was invented in the early 20th century, and the amount of N fertilizer applied in agriculture increased to about 100 Tg N yr^{-1} until the 1990s (Gruber and Galloway, 2008). Generally, less than 65% of N fertilizer applied can be used by crops, and a considerable amount of unused N is released into atmosphere as nitrogenous gases such as ammonia (NH_3), nitrous oxide (N_2O), and nitrogen oxides (NO_x) (Wei et al., 2020). Nitrogenous gases in the atmosphere participate in the formation of cloud and N contained is deposited back to terrestrial (e.g. grassland and forest) and oceanic surface. Due to the huge input of anthropogenic reactive N into the environment, the global N cycle has been strongly accelerated, associated with an increase in the global N deposition from 34 Tg N yr^{-1} in 1860 to 100 Tg N yr^{-1} in 1995 (Galloway et al., 2008). When N compounds are deposited to soils, they are quickly incorporated into an insoluble organic pool resulting in N retention (Lewis and Kaye, 2012). It is assumed that about 50% of deposited N in forests will be biologically and chemically sequestered, and that global N deposition contributed to approximately 10 Tg N yr^{-1} of N retention in 2001–2010 (Zaehle, 2013).

Processes of nitrogen retention in soils highly depends on the species of prevalent inorganic N compounds, e.g. the retention of ammonium (NH_4^+) and nitrate (NO_3^-) largely depends on the biological uptake by microbes and plants, while abiotic reactions with soil organic matter (SOM) contribute mostly to the retention of nitrite (NO_2^-) (Lewis and Kaye, 2012). Nitrite is highly chemically reactive to transition metals and SOM in soils, especially at pH < 7. Isobe et al. (2012) found that 17.8 % of NO_2^- was incorporated into dissolved organic matter within 4 h when applied to a forest soil. Typical products of abiotic NO_2^- reactions with SOM are heterocyclic N compounds, which are receiving more and more interest due to their low biological decomposition rate (Leinweber et al., 2009b). Heterocyclic N, represented by pyrrole and pyridine, is also called black N since it is most often found in fire-affected soils and char. During a wildfire, organic compounds go through condensation and cyclization to form a new pyrogenic organic matter containing black N. However, except for fire-affected soils, black N compounds have also been detected in various natural humic substances (Thorn and Cox, 2009), and the

content of heterocyclic N was found to increase during humification (Abe et al., 2005). Therefore, abiotic reactions of NO_2^- with SOM could play an important role in the long-term N retention in soils.

Nitrite is an intermediate in both nitrification and denitrification, and it exists widely in terrestrial ecosystems. Generally, NO_2^- is regarded as the direct precursor of both biotic and abiotic production of nitric oxide (NO), and its contribution to abiotic nitrous oxide (N_2O) emission has also received attention (Venterea, 2007). Under acidic conditions of pH < 7, NO_2^- combines with a proton to form nitrous acid (HNO_2), which can further react with SOM through N-, C-, or O-nitrosation to form NO, N_2O, and nitrogenous organic compounds (Austin, 1961). Nitrosophenol, *p*-diazoquinone, and o-diazoquinone were identified in the reaction of NO_2^- with phenol under mildly acidic conditions of pH < 7 (Kikugawa and Kato, 1988). Nitrosonaphthol and nitronaphthol were also found as the products of abiotic reaction of NO_2^- with naphthol in soil suspensions at pH 6.5 (Azhar et al., 1989). Rousseau and Rosazza (1998) found that NO_2^--N was incorporated into 7-hydroxy-6-methoxy-1,2(4*H*)-benzoxazin-4-one in the reaction with ferulic acid at pH 2.

The SOM is a complex mixture consisting of both simple molecules and macro polymers that plays a key role in abiotic N fixation. According to ^{13}C-NMR analysis, O-alkyl-C assigned to amides and polysaccharides dominates in SOM, followed by alkyl-C and C/O-substituted alkyl-C, which correspond to chain aliphatic C from lipids and aromatic C from lignin, respectively (Fontaine et al., 2007). It has been reported that aromatic C as well as methylene C and N are reactive sites for nitrosation in the reaction of SOM with NO_2^- (Thorn and Mikita, 2000). Thorn and Mikita (2000) confirmed the formation of nitrophenol, imine, and indophenol from the reactions of fulvic and humic acid with NO_2^- through ^{15}N-NMR analysis. Nevertheless, it is still an open question whether these reactions occur in natural soils or not, and if so, how much they contribute to N retention in natural systems. Therefore, more research is needed to bridge the gap between reactions in chemical assays and N retention in natural soils.

In this study, abiotic N retention resulting from NO_2^-–SOM reactions was investigated in three soils from different land uses (forest, grassland, and agriculture) with different soil pH and organic carbon content (Table 1). Solid-state cross-polarization magic angle spinning (CP-MAS) ^{15}N-nuclear magnetic resonance spectroscopy (NMR), ^{13}C-NMR, and pyrolysis-field ionization (Py-FI) mass spectrometry

were used for structure analysis of immobilized N. Influence of microbial processes on abiotic NO_2^-–SOM reactions was also explored by introducing soil suspension with living soil microbes into the reaction microcosm.

2. Materials and Methods

2.1. Soils and soil parameter analysis

Forest soil (Cambisol) and grassland soil (Cambisol) were sampled from the top 20 cm of Wüstebach catchment (50°30′15″N, 6°18′15″E) and Rollesbroich grassland (50°37′0″N, 6°26′0″E), respectively. These field sites are within the German interdisciplinary research and observation network TERENO (Zacharias et al., 2011). Agricultural soil (Cambic Luvisol) was sampled from the top 30 cm of the Achterwehr field (54°19'05"N, 9°58'38"E), Hohenschulen experimental farm, Kiel, Germany. Three sites in each field were sampled, and soils from each site was immediately air-dried, sieved at 2 mm, and then homogenously mixed.

Soil pH was determined according to the ISO 10390 method (ISO, 2005): 1 M potassium chloride (KCl, analytical grade, VWR, Germany) solution was mixed with freeze-dried soil at a ratio of 1:5 (w/v) for 2 h, centrifuged at 3500 rpm for 20 min, then the suspension was measured with a pH meter (multi 340i, WTW GmbH, Germany). The total N content (TN) and total organic carbon (TOC) were determined using an elemental analyzer (vario EL Cube, Elementar Analysensysteme GmbH, Hanau, Germany) and a multiphase carbon and hydrogen/moisture analyzer (RC612, LECO Instrumente GmbH, Moenchengladbach, Germany), respectively. The contents of iron (Fe) and manganese (Mn) were determined by inductively coupled plasma optical emission spectroscopy (ICP-OES, iCA 7600, Thermo Fisher Scientific, Oberhausen, Germany) after microwave digestion by the mixture of nitric acid (HNO_3, guaranteed reagent, VWR, Germany), hydrofluoric acid (HF, analytical grade, VWR, Germany), and hydrogen peroxide (H_2O_2, analytical grade, VWR, Germany).

The texture of soils used in this study includes silty clay loam (forest soil), sandy loam (agricultural soil), and silty loam (grassland soil), soil pH ranges from 3.6 to 6.0, and SOC content varies from 1.7% to 16.4% (Table 1). Forest soil is characterized by the lowest soil pH and highest SOC content, while agricultural soil by the highest soil pH and lowest SOC content. The ratio of carbon-to-nitrogen (C/N)

in tested soils covers a wide range from 3.2 (grassland soil) to 12.1 (agricultural soil), while contents of Fe and Mn varies from 11.7 to 33.5 and 0.5 to 2.2 mg g^{-1}, respectively.

Table 1. Properties of soils used in this study. Data are presented as mean ± standard error. SOC, soil organic carbon; TN, total nitrogen; WHC, water holding ability; Fe, content of iron; Mn, content of manganese.

Soil	soil texture	pH	SOC[a] (%)	TN[b] (%)	WHC[c] (%)	Fe[d] (mg g^{-1})	Mn[e] (mg g^{-1})
Forest	silty clay loam	3.6 ± 0.0	16.4±1.3	1.46 ± 0.00	137 ± 0.1	29.0 ± 3.0	2.2 ± 0.1
Agriculture	sandy loam	6.0 ± 0.2	1.7 ± 0.2	0.14 ± 0.01	35.0 ± 4.2	11.7 ± 0.2	0.5 ± 0.0
Grassland	silty loam	5.1 ± 0.0	4.1 ± 0.1	1.28 ± 0.10	80.0 ± 4.2	33.5 ± 1.5	1.4 ± 0.4

2.2. Abiotic NO_2^- immobilization in soils and SOM fractions

Abiotic NO_2^- immobilization was analyzed in autoclaved soil samples. To improve the efficiency of autoclaving, 5 g of air-dried soil was rewetted with 5 ml of deionized water in a 22.5-ml glass vial to activate the soil microbes 1 d before autoclaving. Afterwards, the soil was autoclaved for 30 min at 121 °C under a pressure of 300 kPa. The effectiveness of sterilization was confirmed by an agar test where no microbial colony appeared in an agar medium amended with extracts of sterilized soil after 7 d of incubation at room temperature. To achieve significant NMR signals, a much higher amount of sodium nitrite ($NaNO_2$, 10 atom% ^{15}N, analytical grade, VWR, Germany) solution than natural soils was applied to the soil at a ratio of 3.5 µg N g^{-1} soil on a dry weight basis. Then, the glass vial was immediately sealed with an aluminum cap to avoid any microbial contamination, and incubated in a clean bench at room temperature for 4 d.

After incubation, the soil was transferred to a 50-ml sterilized centrifuge tube and mixed with 20 ml of 1 M KCl (analytical grade, VWR, Germany) solution in a clean bench. Before usage, the KCl solution was passed through a 0.2 µm syringe filter to avoid introduction of microbes into the soil. The mixture was centrifuged at 3500 rpm for 20 min to remove the supernatant. The washing procedure with KCl solution was repeated three times to remove remaining ^{15}N compounds that were not fixed by the SOM. In the blank control, the same volume of deionized (MilliQ) water instead of $^{15}NO_2^-$ solution was applied to the soil. After washing, the soil was immediately freeze-dried and stored at room temperature till analysis. To confirm that no microbial contamination occurred during the whole procedure, 0.1 µl

of supernatant after washing was transferred to an agar plate for microbial activity test, and no bacterial colony was observed after 7 d of incubation at room temperature. All the treatments were prepared in triplicate.

To compare the chemical N fixation ability of fulvic acid and humus (i.e. the sum of humic acid and humin), the soil was fractionated with hydrochloric acid (HCl, VWR, Germany) and hydrofluoric acid (HF, VWR, Germany): firstly, soil samples were treated with 1 M HCl for 2 h at room temperature to remove inorganic carbon, then washed with deionized water until a pH 4-5 was reached, and afterwards freeze-dried; secondly, the soil was treated three times with a mixture of 35% HF and 5% HCl for about 16 h at room temperature to separate fulvic acid and humus; then, fulvic acid in the mixed solution of HF and HCl was recovered by solid phase extraction (Bond Elut-PPL, 500 mg, 6 mL, VWR, Germany); lastly, the remaining humus after HF-HCl treatment was washed with deionized water to pH 4-5, and then freeze-dried for further analysis (Stevenson, 1995; Wei et al., 2017).

Both C and N content and isotope analysis were performed with an elemental analyzer coupled to an isotope-ratio mass spectrometer (EA-IRMS, Flash EA 2000 and Delta V Plus; Thermo Fisher Scientific, Bremen, Germany). For organic C content and its $\delta^{13}C$ value determination, 0.2–5 mg of sample (^{15}N enriched bulk soil, fulvic acid or humus) equivalent to about 100 µg C was used, while 0.1–5 mg of sample containing approximately 35 µg N for determination of organic nitrogen content and its ^{15}N enrichment. The N immobilization ratio (R_{im}) in soils was calculated as the proportion of ^{15}N immobilized in soil organic nitrogen (SON) of the total applied ^{15}N:

$$R_{im}\ (\%) = \frac{(^{15}N_{enr} \times SON_{enr} - {}^{15}N_{loc} \times SON_{loc}) \times M_{soil}}{^{15}N_{tot}} \times 100\% \qquad \text{(Equation 1)}$$

where $^{15}N_{enr}$ and $^{15}N_{loc}$ (atom %) denote the ^{15}N enrichment of SON in $^{15}NO_2^-$ amended and blank control treatment, respectively; SON_{enr} (%) is the SON content in $^{15}NO_2^-$ amended soil, and SON_{loc} is the SON content in the blank control; M_{soil} (5 g freeze-dried soil) represents the total amount of soil used in each treatment; $^{15}N_{tot}$ (17.5 µg) is the total amount of ^{15}N applied to the soil. The SOC content of the soil, yields of fulvic acid and humus, as well as their $\delta^{13}C$ value, are listed in Table 2.

2.3. Structure analysis of immobilized organic N compounds

To enhance the intensity of ^{15}N-NMR signals of immobilized organic N compounds, forest humus (FOM) and grassland humus (GOM) were reacted with $Na^{15}NO_2$ (99 atom% ^{15}N, analytical grade, VWR, Germany) for a second time. To be precise, 0.4 g of FOM or GOM was mixed with 0.2 g of $Na^{15}NO_2$ dissolved in 10 ml of sterilized water in a sterilized 25-ml centrifuge tube, and incubated in a clean bench for 6 d at room temperature. Instead of sterilized water, 10 ml of soil suspension with living microbes obtained from a Cambisol soil planted with *Aloe arborescens* was used in microbial treatments to test the effect of soil microbes on the abiotic N immobilization. For the preparation of soil microbial suspension, 20 g of fresh soil from the rhizosphere of *Aloe arborescens* was suspended in 40 ml of MilliQ water, and the mixture was incubated in a shaker at room temperature for 24 h, afterwards the suspension was passed through a 80–120 µm Whatman filter paper to remove soil particles and permit most soil microbes remine in the suspension. Humus instead of original soils was used in this experiment, the live soil organisms had been sterilized and the original soil structure had been destroyed, therefore, limitations of inoculation of soil microbial suspension from one soil to other ones were neglected. After reactions of humus with $Na^{15}NO_2$, the mixture was centrifuged at 4000 *g* for 20 min, and the liquid phase was carefully decanted into another 25-ml sterilized tube. Both liquid and solid phase were freeze-dried for further analysis.

The solid-state ^{15}N- and ^{13}C-NMR spectra were obtained with a Bruker Advance III HD 400 MHz Wideboard (Bruker, Billerica, Massachusetts, United States) operating at resonance frequencies of 40.56 MHz and 100.63 MHz, respectively. 0.3-0.5 g of samples were placed into zirconium rotors of 7 mm and 4 mm O.D. with KEL-F-caps for ^{15}N- and ^{13}C-NMR analysis, respectively. The cross polarization magic angle spinning (CP-MAS) technique was applied with a spinning speed of the rotor at 6 kHz and 14 kHz for ^{15}N- and ^{13}C-NMR spectra, respectively, with a pulse delay of 200 ms. A ramped 1H-pulse was used during a contact time of 1 ms in order to circumvent spin modulation of Hartmann-Hahn conditions. A contact time of 1 ms and a 90° 1H-pulse width of 3.5 µs were used for all spectra. The ^{15}N-chemical shifts were calibrated with glycine (-346.7 ppm) against nitromethane (0 ppm), while the ^{13}C-chemical shifts were calibrated with glycine (176.04 ppm) against tetramethylsilane (= 0 ppm). The relative intensities of the peaks were obtained by integration of the specific chemical shift ranges with

198 an integration routine with MestreNova 10 (Mestrelab research, Santiago de Compostela, Spain). The
199 ^{15}N- and ^{13}C-NMR spectra were assigned to corresponding N- or C-compounds according to Knicker
200 (2011b).

201 For pyrolysis-field ionization mass spectrometry (Py-FIMS) analysis, about 0.4 milligrams of the
202 samples were degraded by pyrolysis in the ion source (emitter: 4.7 kV, counter electrode -5.5 kV) of a
203 double-focusing Finnigan MAT 95. Samples were heated in a vacuum of 10^{-4} Pa from 50 °C to 650 °C,
204 in temperature steps of 10 °C over a time period of 15 minutes, recording spectra over the mass range
205 15 to 900 m/z for each of the 60 temperature steps. Between magnetic scans the emitter was flash heated
206 to remove residues of pyrolysis products (Leinweber et al., 2009a; Schnitzer and Schulten, 1992).

207

208 2.4 Statistical analysis

209 Triplicates are low to reliably test normal distribution and inhomogeneity of variance, therefore,
210 one-way analysis of variance (ANOVA) with Tukey-B test was conducted using OriginPro 8.0
211 (Originlab Corporation, Wellesley Hills, MA, USA), which is less susceptible to inhomogeneity and
212 non-normality (Reichel et al., 2018). The significance threshold for the comparisons was set at $p = 0.05$.

213

214 **3. Results**

215 3.1. Abiotic NO_2^- retention

216 Recovered fulvic acid and humus accounted for 0.3-2.1% and 39.3-78% of the total SOC,
217 respectively, and $^{15}NO_2^-$ application did neither significantly ($p > 0.05$) alter their proportion nor their
218 ^{13}C enrichment (Table 2). Yield of fulvic acid was positively correlated to the SOC content in bulk soils,
219 and decreased in the order of forest soil, grassland soil, and agricultural soil.

220

221 **Table 2.** The soil organic carbon (SOC) content and its $\delta^{13}C$ value in bulk soils, fulvic acid, and
222 humus before and after $^{15}NO_2^-$ application.

		Bulk soil		Fulvic acid		Humus	
		SOC (%)	δ^{13}C vs. PDB (‰)	Yield (% SOC-C)[a]	δ^{13}C vs. PDB (‰)	Yield (% SOC-C)	δ^{13}C vs. PDB (‰)
Forest	before	16.4 ± 1.3	-25.9 ± 0.2	2.1 ± 0.0	-26.7 ± 0.1	76.6 ± 0.5	-25.5 ± 0.4
	after	17.4 ± 3.5	-26.0 ± 0.1	1.6 ± 0.0	-26.7 ± 0.1	78.0 ± 4.4	-25.9 ± 0.3
Grassland	before	4.1 ± 0.1	-28.4 ± 0.1	1.2 ± 0.0	-28.1 ± 0.1	43.6 ± 0.3	-29.7 ± 0.2
	after	4.2 ± 0.3	-28.4 ± 0.2	1.5 ± 0.0	-28.4 ± 0.0	46.8 ± 0.7	-29.6 ± 0.2
Agriculture	before	1.7 ± 0.2	-27.6 ± 0.5	0.5 ± 0.0	-27.3 ± 0.0	46.5 ± 1.0	-28.7 ± 0.2

	after	1.5 ± 0.1	-27.9 ± 0.0	0.3 ± 0.0	-27.3 ± 0.0	39.3 ± 7.8	-29.0 ± 0.1

Note:

[a] calculated as the percentage of the total carbon content in fulvic acid to the soil organic carbon (SOC) in bulk soil. No significant differences of SOC content, fulvic acid and humus yields, as well as their $\delta^{13}C$ value were found before and after $^{15}NO_2^-$ application.

After 4 d of incubation under sterilized conditions, 6.3–7.6% of NO_2^- was immobilized in the soil, and there was no significant ($p > 0.05$) difference in N retention among the three types of soils and land uses despite their distinct SOC content (Figure 1a). In contrast, N immobilization varied largely in different SOM fractions. Even though fulvic acid only accounted for 0.3–2.1% of the SOC (Table 2), the ^{15}N enrichment of fulvic acid was 2–3 times higher than that of the corresponding humus and bulk soil (Figure 1b), which indicates that fulvic acid is highly reactive to NO_2^-.

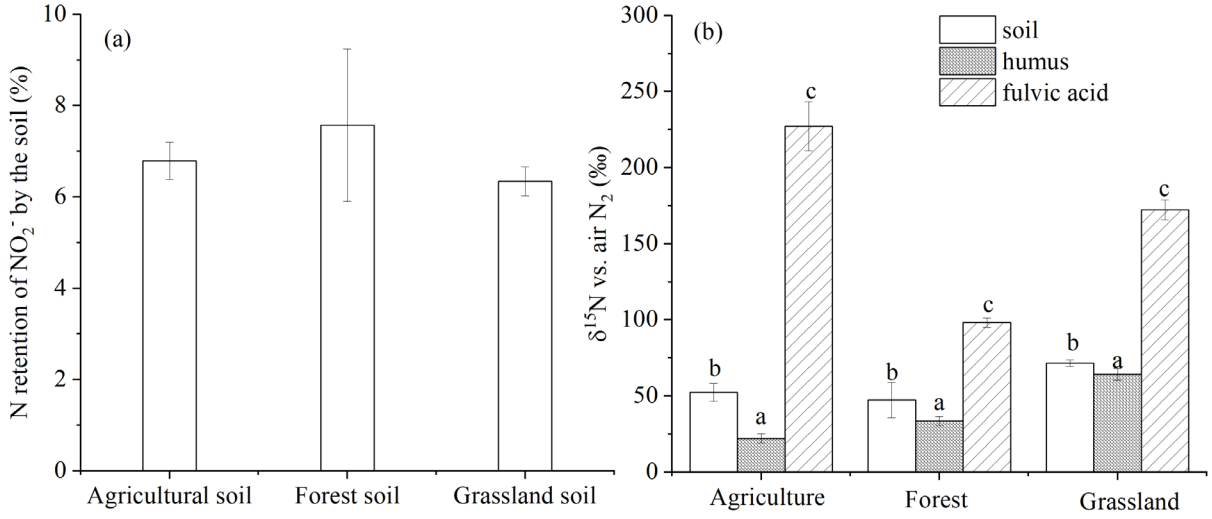

Figure 1. Abiotic N retention of NO_2^- in agricultural, forest, and grassland soil (a) and $\delta^{15}N$ values of bulk soil, fulvic acid, and humus in $^{15}NO_2^-$ amended soils (b). Different letters in (b) indicate significant ($p < 0.05$) differences of ^{15}N enrichment among bulk soil, fulvic acid, and humus in the same land use type.

3.2. ^{15}N-NMR spectroscopy of immobilized N compounds

According to the solid-state CP-MAS ^{15}N-NMR spectra, the major peak from -230 to -285 ppm, representing amide-N, accounted for 49–66% of the total N in $^{15}NO_2^-$ amended humus, while the peak from 50 to -50 ppm, representing nitrate-N, nitro-N, and oxime-N, accounted for 10–30% of the total N

in $^{15}NO_2^-$ amended humus (Figure 2). The downfield shoulder from 50 to 10 ppm represents the monoximes, and the peak at -2 ppm represents nitrate (Figure 2). The pyridine and nitrile-N signals generally occur at frequency from -50 to -180 ppm. No pyridine was found in any treatment, while a nitrile peak from -100 to -160 ppm was found in the solid phase of $^{15}NO_2^-$ treated forest humus (Figure 2). However, black N represented by pyrroles at the frequency of -180 to -230 ppm was found in $^{15}NO_2^-$ amended treatments (Figure 2). The peak from -230 to -285 ppm corresponds with amides. Different from microbial amides in natural humus that peaked at -257 ppm, chemically formed amide-N peaked at around -270 ppm in NO_2^- treated humus (Figure 2).

Even though GOM was characterized by amide-N and FOM by both amide- and pyrrole-N, the composition of the newly fixed N components after $^{15}NO_2^-$ amendment was similar in the SOM of both soils (Figure 2). Due to the higher C content of forest humus (Table 2), about 6 μg ^{15}N kg^{-1} OM more was fixed by FOM than that by GOM, most of which in the form of amide-, nitro-, and pyrrole-N (Table 3). After $^{15}NO_2^-$ amendment, the liquid phase contained 12–20% less nitro/oxime-N and 14–17% more amide-N compared with the solid phase, while the contents of other products were similar in the two phases (Figure 2, Table S1). Notably, neither the forms of abiotic SON products nor their quantity was affected by the introduction of microbes (Figure 2, Table S1).

Table 3. Content of different N-compounds (μg ^{15}N kg^{-1} OM) and C-compounds (mg C kg^{-1} OM) in grassland (GOM) and forest (FOM) humus before and after $^{15}NO_2^-$ application.

Range (ppm)	FOM[a]			GOM[b]		
	-	$+^{15}NO_2^-$ [c]	$+^{15}NO_2^- + M$ [d]	-	$+^{15}NO_2^-$	$+^{15}NO_2^- + M$
^{15}N-NMR						
50 to -50 (nitro/nitrate-N)	-	7.45		-	4.15	4.7
-100 to -180 (pyridine/nitrile-N)	-	0.74		-	1.54	1.18
-180 to -230 (pyrrole-N)	0.34	2.26		-	1.58	1.43
-230 to -285 (amide-N)	0.6	12.28		0.78	9.45	9.19
-285 to -320 (amino-N)	-	1.92		-	1.53	1.51
Total	0.94	24.65		0.78	18.26	18.01
^{13}C-NMR						

225–185 (aldehyde-/ketone-C)	9.01	5.83	7.35	3.10	4.10	7.08
185–160 (carboxyl-/amide-C)	41.01	34.40	36.67	20.23	26.81	27.50
160–140 (aryl-O-/aryl-N-C)	35.21	32.18	34.92	12.03	13.27	15.12
140–110 (aryl-C/olefinic-C)	213.02	259.44	265.50	35.46	47.60	50.37
110–90 (acetal-/ketal-/aromatic-C)	36.00	33.41	30.43	17.76	21.43	20.86
90–60 (alkyl-O-C)	87.07	78.30	65.59	56.01	78.95	76.70
60–45 (aliphatic C-N, methoxyl-C)	36.54	28.39	27.17	30.63	38.59	37.27
45–0 (Alkyl-C)	123.90	111.06	115.38	109.48	171.29	167.11

Note:

[a] Forest humus;

[b] Grassland humus;

[c] NO_2^- amendment;

[d] NO_2^- and microbes amendment.

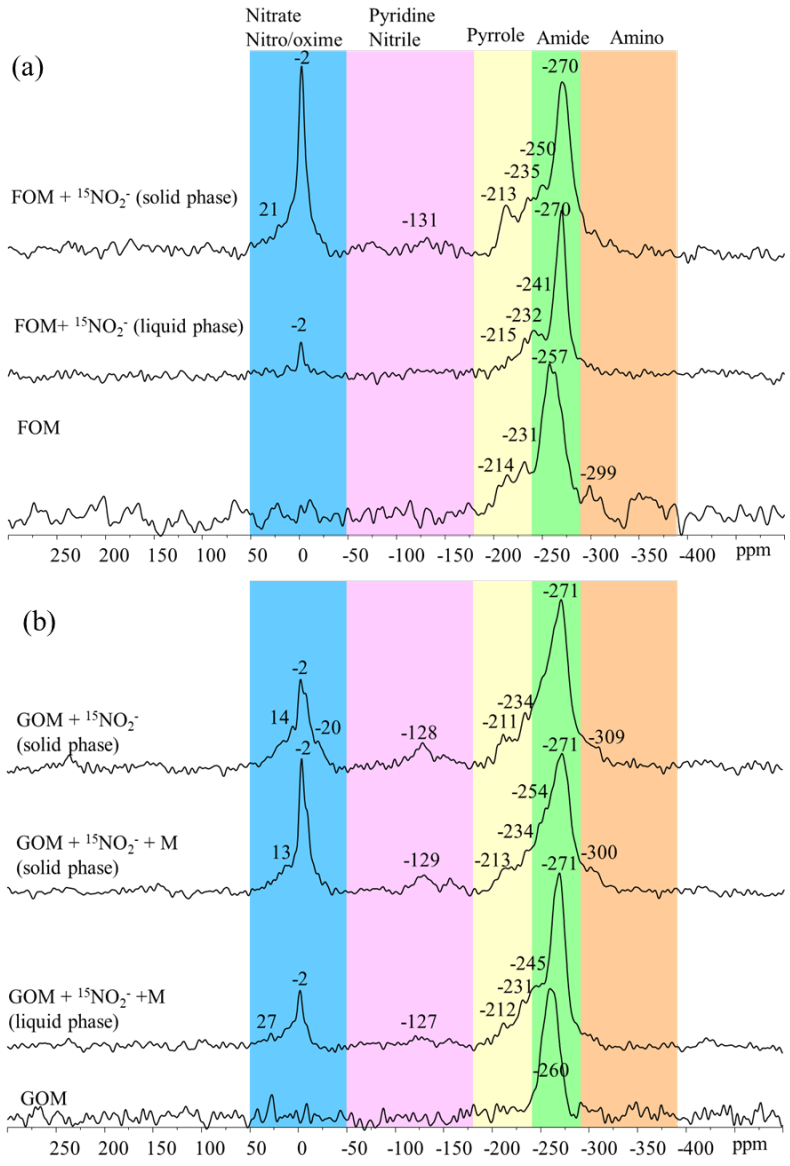

Figure 2. Solid-state CP-MAS ^{15}N-NMR spectra of forest humus (FOM, a) and grassland humus (GOM, b) with or without amendment of $^{15}NO_2^-$ and microbes (M).

3.3. Impact of N immobilization on SOC structure revealed by ^{13}C-NMR

Eight groups of SOC were detected according to ^{13}C-NMR, i.e. aldehyde-/ketone-C (225–185 ppm), carboxyl-/amide-C (185–160 ppm), aryl-O-/aryl-N-C (160–140 ppm), aryl-C/olefinic-C (140–110 ppm), acetal-/ketal-/aromatic-C (110–90 ppm), alkyl-O-C (90–60 ppm), aliphatic C-N/methoxyl-C (60–45), and Alkyl-C (45–0 ppm) (Figure 3). Grassland humus was dominated by alkyl-C, which accounted for more than 30% of the total ^{13}C-NMR signal, followed by alkyl-O-C and aryl- and olefin-C (Figure 3a). By contrast, aryl- and olefin-C, accounting for more than 40% of the total ^{13}C-NMR signal, were the major SOC species in forest humus, followed by alkyl-C and alkyl-O-C (Figure 3b). In parallel to the

formation of amide and pyrrole revealed by ^{15}N-NMR, the amendment of $^{15}NO_2^-$ significantly increased the content of aryl- and olefin-C by more than 22% in both forest and grassland humus (Table 3).

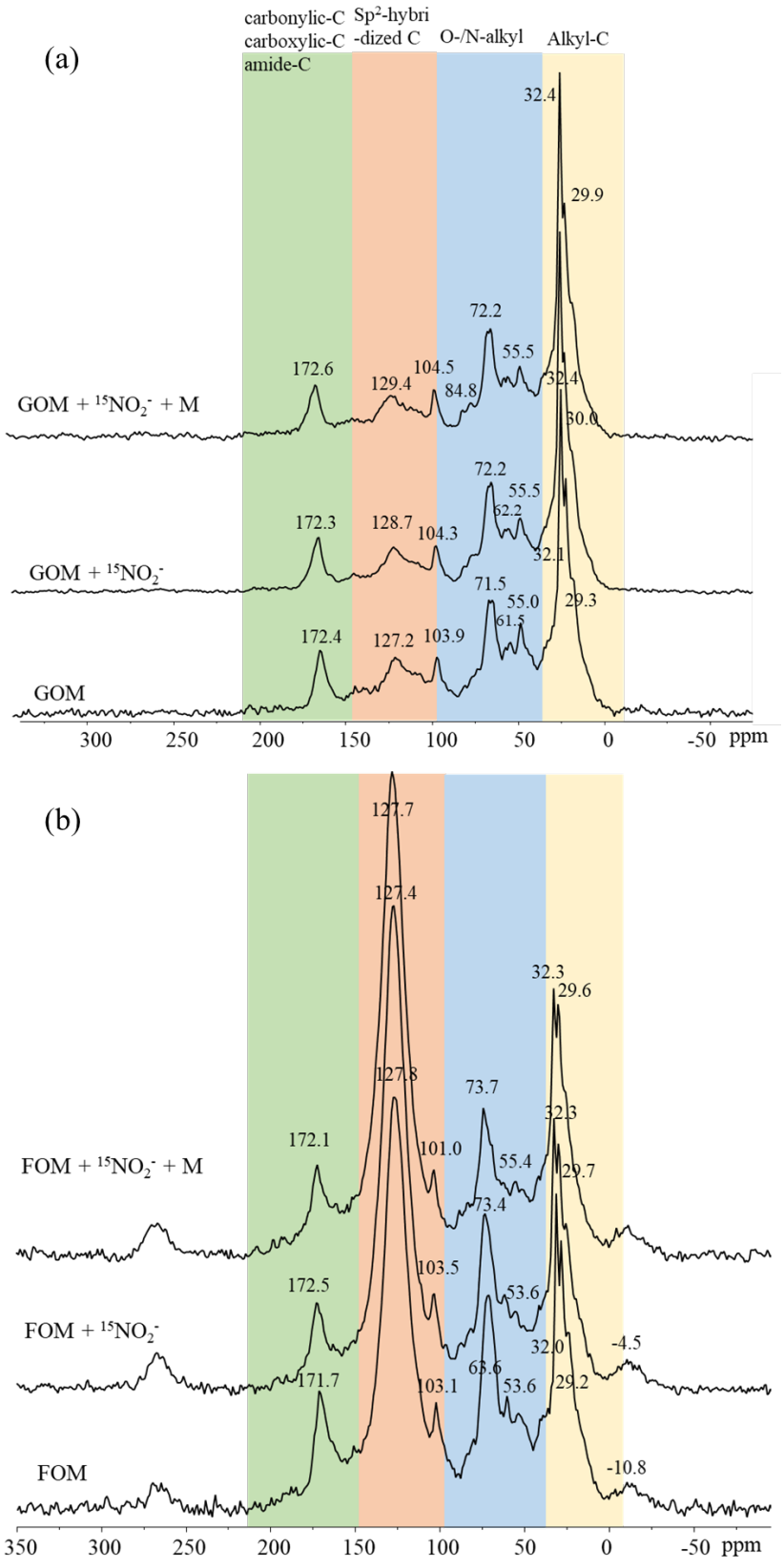

Figure 3. Solid-state CP-MAS ^{13}C-NMR spectra of grassland humus (GOM, a) and forest humus (FOM, b) with or without amendment of $^{15}NO_2^-$ and microbes (M).

3.4 Pyrolysis-field ionization (Py-FI) mass spectrometry of immobilized N compounds

The summed and averaged Py-FI mass spectra of forest and grassland OM, without and with addition of soil microbes, all showed intensive spectra in the mass range *m/z* 30 to > 780 (Figure 4). Mass signals in the lower mass range indicate the presence of carbohydrates (e.g., *m/z* 98, 126, 163). Most prominent in the higher mass range were signals from homologues of *n*-C_{16} to *n*-C_{34} fatty acids (*m/z* 256, 284, …. 508) and alkyl monoesters (*m/z* 676, 704, 732 and 760). Less prominent signals can be assigned to compound classes that are always found in soil organic matter, such as phenols and lignin monomers, lignin dimers, lipids, alkyl aromatic sterols, peptides and suberin. The comparison of thermograms of total ion intensity (TII) indicates differences between FOM and GOM, with the latter showing much higher ion intensities almost over the whole temperature range. These differences between sites obviously were much more pronounced than differences between samples with and without microbes, which had rather similar TII curves and spectral patterns.

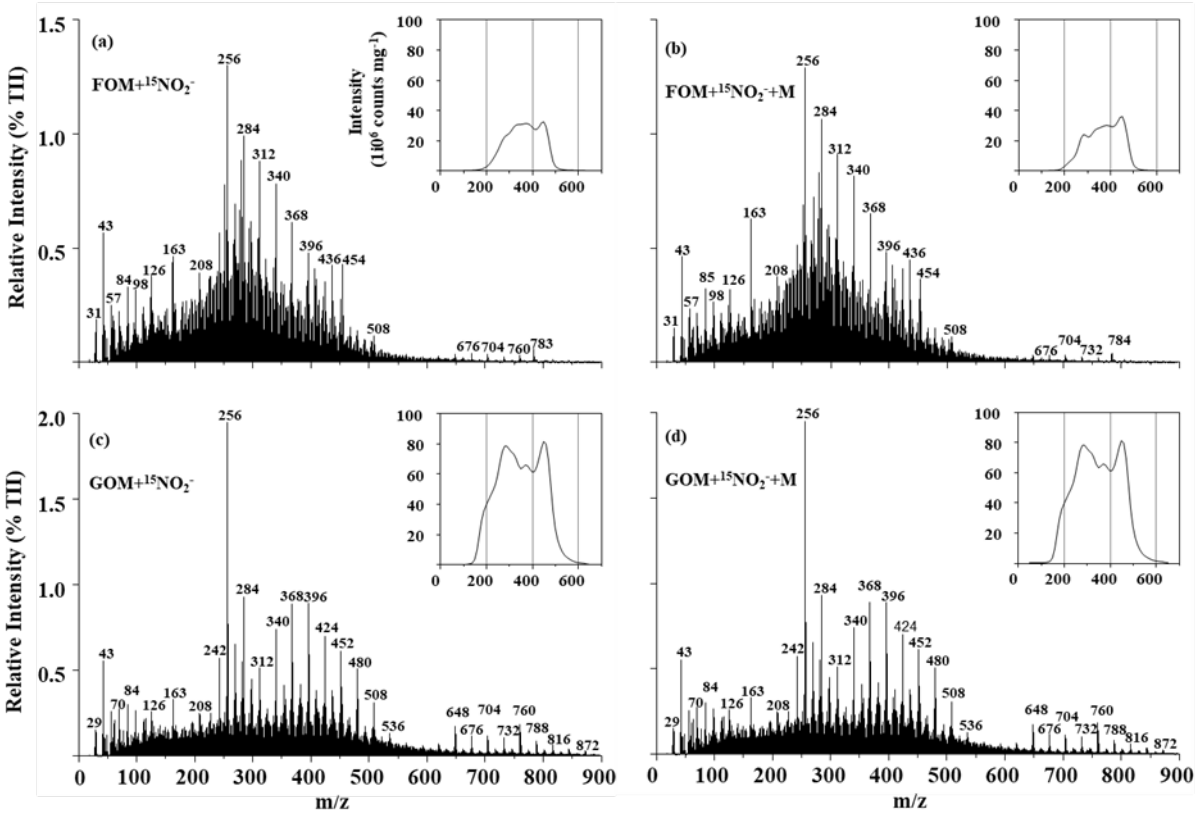

Figure 4. Summed and averaged Py-FI mass spectra of sterile forest humus with $^{15}NO_2^-$ (FOM+$^{15}NO_2^-$), microbially inoculated forest humus with $^{15}NO_2^-$ (FOM+$^{15}NO_2^-$+M), sterile grassland humus with $^{15}NO_2^-$ (GOM+$^{15}NO_2^-$), and microbially inoculated grassland humus with $^{15}NO_2^-$ (GOM+$^{15}NO_2^-$+M).

Forest humus had a much higher proportion of substances thermally stable at 450 °C, which were bound in soil aggregates, while grassland humus was characterized by a higher proportion of organic compounds with lower thermal stability at 250-300 °C (Figure 5). A multivariate statistical evaluation, first using all *m/s* signals (not shown), and subsequently only those with significant differences in ion intensities (Figure 6), showed a clear separation of the samples according to their origin (forest vs. grassland), and within the groups of same origin, with and without microbes. Along PC 1, which accounted for 96% of the difference, the samples were separated according to origin, while separation according to microbial influence occurred along PC 2, which accounted for only 1.1 % of the overall differences among spectra. Thus, it is clear that the site differences were much more pronounced than the differences between treatments.

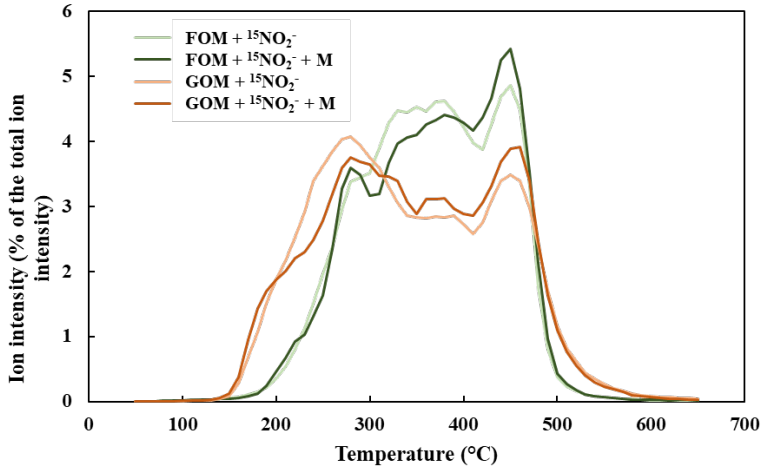

315

316 **Figure 5**. The thermal curves of the ion intensities in non-inoculated forest humus with $^{15}NO_2^-$
317 (FOM+$^{15}NO_2^-$), inoculated forest humus with $^{15}NO_2^-$ (FOM+$^{15}NO_2^-$+M), non-inoculated grassland
318 humus with $^{15}NO_2^-$ (GOM+$^{15}NO_2^-$), inoculated grassland humus with $^{15}NO_2^-$ (GOM+$^{15}NO_2^-$+M). The
319 total ion intensity (TII) always correlates closely with the organic content, therefore TII% represents
320 relative proportions of the organic.

321

322

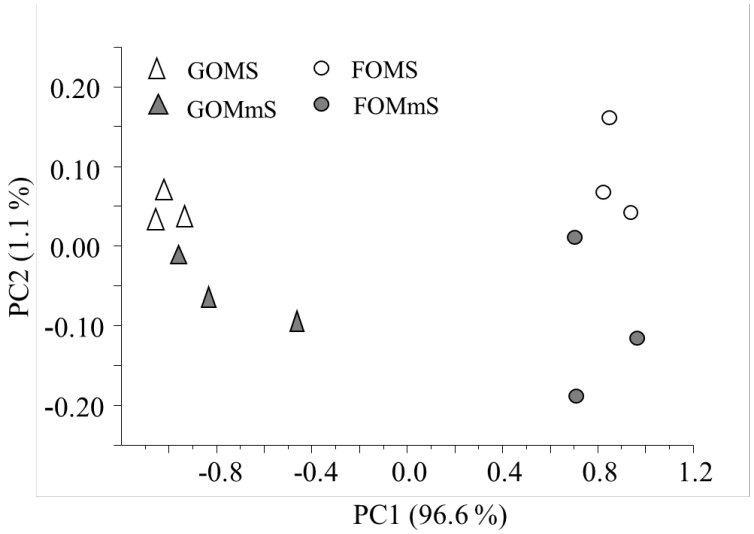

323 **Figure 6.** Principal component analysis of Py-FI Mass spectra using the 177 *m/z* values with the most
324 significant differences between the four samples according to univariate Wilks' lambda.

325

326 The volatile matter in the range of about 55 to 75% (w/w) confirms that the samples were mostly
327 organic, which is not surprising given the HCl/HF treatments. Overall, the samples from grassland soil
328 yielded a much larger TII than those from the forest soil (Table 4). The assignment of marker signal to

329 important compound classes of SOM showed that lipids and alkyl aromatics were the most abundant
330 compound classes in samples from the forest soil, while free fatty acids and lipids were most abundant
331 in samples from the grassland soil. According to this assignment, the order of abundances was
332 phenols/lignin monomers > free fatty acids > carbohydrates > peptides (grassland), and alkyl aromatics >
333 phenols/lignin monomers > carbohydrates > peptides. Significantly larger TII proportions were obtained
334 for phenols/lignin monomers, lignin dimers, lipids, alkyl aromatics, peptides at the expense of suberin
335 and free fatty acids in the samples from the forest compared to the samples from the grassland soil. An
336 influence of microbial inoculation is reflected by significantly larger proportions of carbohydrates at the
337 expanse of suberin in the GOMmS sample (Table 4).

Table 4. Data evaluation of Py-FI mass spectra: Volatile matter (VM, % w/w) and total ion intensities (TII, 10^6 counts mg^{-1}), and proportions of important compound classes in FOM (forest humus), FOMm (inoculated forest humus), GOM (grassland humus) and GOMm (inoculated grassland humus). (Data are shown as mean (standard deviation), CHYDR = carbohydrates, PHLM = phenols and lignin monomers, LDIM = lignin dimers, LIPID = lipids, ALKY = alkyl aromatics, NCOMP = heterocyclic nitrogen containing compounds, PEPTI = peptides, SUBER = suberin, FATTY = free fatty acids).

Treatment	VM	TII	CHYDR	PHLM	LDIM	LIPID	ALKY	NCOMP	PEPTI	SUBER	FATTY
FOM	54.6 (8.4)	684.9 (65.3)	5.1 (0.7)	8.2 (0.8)	3.7 (0.4)	9.4 (0.2)	9.2 (0.1)	1.5 (0.1)	4.1 (0.3)	0.9 (0.0)	6.8 (0.5)
FOMm	58.0 (13.6)	691.0 (42.6)	4.8 (0.4)	7.9 (0.7)	4.0 (0.5)	9.4 (0.3)	9.4 (0.6)	1.5 (0.1)	3.8 (0.2)	0.9 (0.1)	7.0 (1.1)
GOM	61.7 (3.1)	2255.0 (393.2)	3.8 (0.1)	4.7 (0.2)	2.1 (0.0)	7.6 (0.0)	5.2 (0.2)	1.6 (0.1)	3.2 (0.1)	1.8 (0.0)	12.1 (0.3)
GOMm	74.6 (9.3)	2113.4 (125.5)	4.1 (0.1)	5.6 (0.5)	2.5 (0.4)	7.8 (0.3)	6.1 (0.6)	1.7 (0.1)	3.5 (0.0)	1.6 (0.0)	11.6 (1.7)

Detecting ^{15}N enrichment in individual molecules is outmost complicated since the label eventually is distributed among many single molecules at completely unknown quantities. Nevertheless, by using the instrument in high resolution mode, it was possible to find indications for the incorporation of nitrite-N into organic N compounds, depending on the presence of microbes. The mass distributions of nominal mass *m/z* 84 in Figure 7 shows peaks of two N-compounds (84.04 and 84.07) that are formed by pyrolysis of peptides. Given that these peaks originated from the source ^{15}N-nitrite, a peak should appear at 85.037 with the intensity of 5 $\times 10^6$. In the spectrum of GOMS sample this is within the noise level, but in the spectrum of GOMmS a distinct peak is clearly visible at *m/z* 85.037. This indicates that in the inoculated sample some of the ^{15}N-nitrite had been transformed into glutamine/glutamic acid, but no so in the non-inoculated sample.

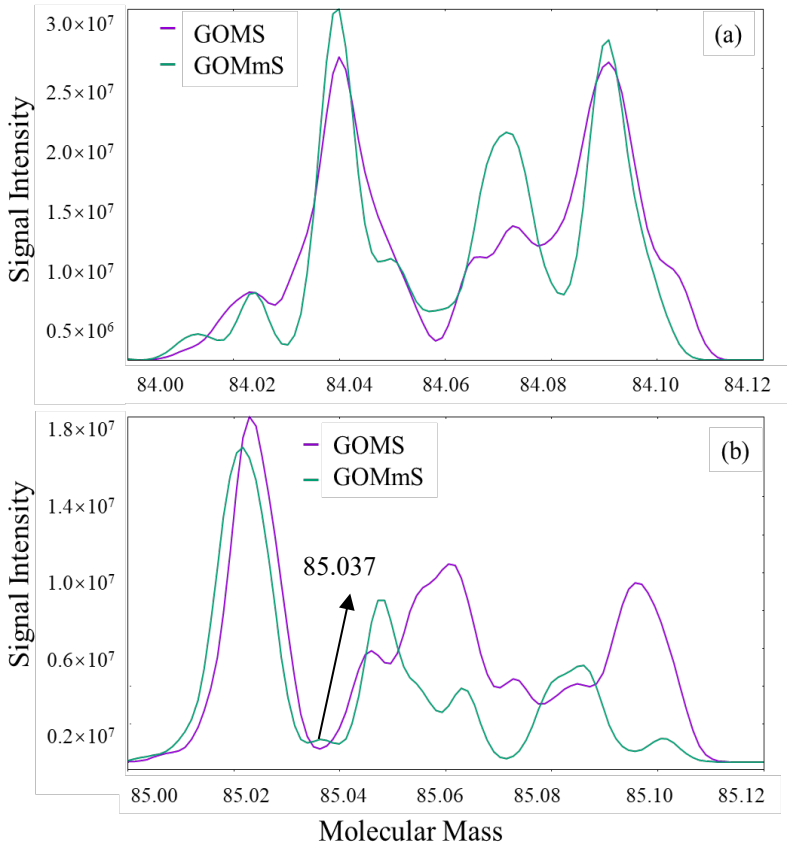

Figure 7. Highly resolved spectral pattern in the mass range *mz* 84 to 84.12 (a) and 85 to 85.12 (b) of ^{15}N-nitrite treated grassland soil samples with (GOMmS) and without (GOMS) microbial inoculation.

4. Discussion

4.1 Mechanisms involved in chemical N immobilization

In this study, $^{15}NO_2^-$ was immobilized in soil humus as nitro-, nitrile-, pyrrole-, amide-, and amino-N compounds involving a series of organic chemical reactions (Table 3). At pH < 7, NO_2^- combines with a proton to form nitric acid (HNO_2) and further reacts with aromatic compounds to form nitrosophenols through nitrosation, and oximes derived from the nitrosophenols via tautomeric rearrangement (Reaction 1) (Thorn and Mikita, 2000; Wei et al., 2019). After nitrosation, also nitro compounds can be formed through the oxidation of the nitroso-compounds (Reaction 2) (Thorn and Mikita, 2000).

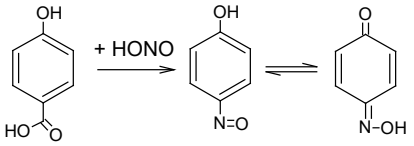

[1]

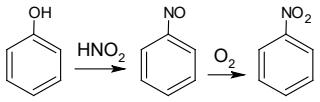

[2]

Nitriles can be formed through Beckmann fragmentation of ketoximes and quinone monoximes (Reactions 3 and 4) at acidic conditions of pH < 7, while pyrroles and pyridines can be formed through Knorr pyrrole synthesis (Thorn et al., 1992; Thorn and Mikita, 2000). The hydrolysis of nitriles (Reaction 5) or the Beckmann rearrangement of oximes (Reaction 6) lead to the formation of amides (Thorn and Cox, 2016).

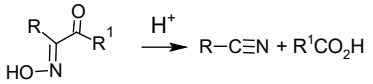

[3]

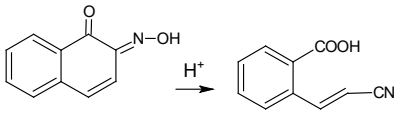

[4]

382 $$RCN \xrightarrow{H_2O} RCONH_2 \quad [5]$$

383 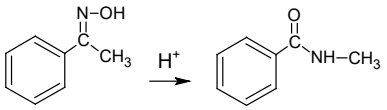 [6]

384

385 Thorn and Mikita (2000) investigated the reaction of NO_2^- with International Humic Substance
386 Society peat humic acid using liquid-phase ACOUSTIC ^{15}N-NMR; nitrosophenol- and oxime-N
387 represented about 76% of the total products, while amides only accounted for about 7%. In the present
388 study, the samples were reacted for 6 d, which was much longer than the formerly used 24 h, so there
389 was sufficient time for oximes to undergo the following Beckmann rearrangement, Beckmann
390 fragmentation, and hydrolysis to finally form amides. This could explain the much higher content of
391 amides in this study. In addition, nitro compounds instead of nitroso compounds were prevalent in this
392 study, because nitroso compounds are not stable and can be easily oxidized to nitro compounds or
393 transformed to amides at pH < 7. By contrast, Rousseau and Rossazza (1998) reported the formation of
394 2-methoxy-4,6-dinitrophenol and 2-methoxy-6-nitrophenol from the reaction of NO_2^- with ferulic acid,
395 which resulted from the oxidation of their corresponding nitrosophenols.

396

397 4.2 Factors affecting abiotic N immobilization

398 The SOC content and pH are generally regarded as main factors controlling the chemical
399 immobilization of NO_2^- in soils (Dail et al., 2001). Under acidic condition of pH < 7, NO_2^- can be
400 protonated to HNO_2 which is highly reactive to SOM and transition metals, hence it is thought that
401 chemical NO_2^- immobilization is favored by acidic pH (Riordan et al., 2005). But on the other hand, the
402 competitive reaction of chemodenitrification of nitrite is also higher at lower pH, leading to higher
403 gaseous N losses in the form of NO, NO_2 and HONO (Su et al., 2011; VanCleemput and Samater, 1996).
404 Islam et al. (2008) found that abiotic NO_2^- immobilization did not occur any more when the pH increased
405 to 8.

406 In addition, the content of SOC, i.e., the substrate of abiotic NO_2^-–SOM reactions, was found to be
407 significantly positively correlated with the chemical N retention in various soils (Fitzhugh et al., 2003b).
408 However, the N retention in forest soil was not significantly higher compared with agricultural and

409 grassland soils in spite of its markedly lower pH and higher C content in the present study (Figure 1),
410 indicating that not only the amount of SOC but also its quality play an important role in abiotic N
411 immobilization (Wei et al., 2020).

412 The content of transition metals, including Fe and Mn in mineral aggregates, is another factor
413 controlling the chemical reactions of NO_2^- with SOM. Transition metals in mineral aggregates can
414 quickly reduce NO_2^- to nitrous oxide (N_2O), nitric oxide (NO), and dinitrogen (N_2), therefore, higher
415 contents of transition metals generally lead to larger emission of nitrogenous gases but lower N
416 immobilization (Wei et al., 2020). The abiotic N retention of NO_2^- in this study is comparable to the 10%
417 N retention found in Canton soils at pH 3.9–5.0 (Dail et al., 2001), but substantially lower than the 20%
418 in a sandy loam soil with SOC content of 6% and pH of 3.8–4.0 (Islam et al., 2008) and the 65–80% in
419 an Inceptisol soil with SOC content of 30% and pH of 3.4–3.9 (Fitzhugh et al., 2003a). The lower N
420 retention ratio in this study compared with that in Islam et al. (2008) and Fitzhugh et al., (2003a) could
421 be explained by its much higher transition metal (Fe and Mn) contents.

422 Forest soil was finer textured with silty clay loam compared to that of agricultural and grassland
423 soils (Table 1), while no significant ($p > 0.05$) differences of chemical N retention were found among
424 the three soils (Figure 1). Similarly, chemical reactions of NO_2^- with SOM were not significantly
425 affected by soil texture according to Islam et al. (2008) and Fitzhugh et al., (2003a, b). Different from
426 ammonium immobilization dominated by physical adsorption by soil mineral surfaces, NO_2^-
427 immobilization was controlled by it chemical reactions occurring quickly within several minutes to
428 hours, and reactive points are more than enough regardless of their soil texture (Nelson, 1967).

429 Fulvic acid is composed of aromatic macromolecules with lower molecular weight and aromaticity
430 than humic acid and humin (Stevenson, 1995). Furthermore, it is generally characterized by relatively
431 higher C/N ratio, more alkyl-C and carboxyl-C than humic acid (Gondar et al., 2005; Weber and Wilson,
432 1975). These characteristics make fulvic acid much more reactive to NO_2^- than dissolved organic matter,
433 humic acid, and humin (Wei et al., 2017). Due to the high reactivity of fulvic acid, its chemical reaction
434 with NO_2^- was found to contribute the most to abiotic N immobilization and also to abiotic N_2O emission
435 in soil (Wei et al., 2017).

436

437 4.3 Significance of abiotic N immobilization in soil

438 Amide- and amino-N are the most abundant N species in natural soils (Knicker, 2011b). In the
439 present study, we demonstrated that chemical reactions of NO_2^- and SOM introduced amide and amino
440 compounds to the soil humus fraction (Figure 2). This is possible since aromatic C compounds derived
441 from lignin offer abundant reactive sites for the incorporation of NO_2^--N into SOM to form amides, as
442 already proposed by Schmidt-Rohr et al. (2004).

443 Black N, represented by pyrrole and pyridine, is abundant in burned soils, peat, and biochar (Thorn
444 and Cox, 2009), therefore, it was proposed that the high temperature during burning may be a
445 prerequisite for the formation of black N (Knicker, 2007). However, our results proved that chemical N
446 immobilization at ambient temperature could be an alternative pathway of black N formation, especially
447 during periods of NO_2^- accumulation in soils with high aromatic C content (Table 3). It was reported
448 that the content of black N was positively correlated with the aromaticity of SOM and increased during
449 humification (Abe et al., 2005; Gillespie et al., 2009). Therefore, a series of chemical reactions between
450 aromatic C and reactive N compounds during humification could contribute to the formation of black N
451 compounds in soil, and thereby add substantial variety to the large number of biologically produced
452 heterocyclic organic N compounds (Leinweber et al., 2013).

453 The formation of oximes is the key step for N incorporation into SOM, not only in the reactions of
454 SOM with NO_2^-, but also with hydroxylamine, ammonia, and nitric acid, while nitriles and amides are
455 the products of the following Beckmann rearrangement or fragmentation (Thorn et al., 1992; Thorn and
456 Cox, 2016; Thorn and Mikita, 1992). Amides were found as the main forms of fixed N in our study,
457 while black N, including indoles and pyrroles, was mainly produced from chemical reactions of fulvic
458 and humic acids with ammonia through the polymerization of amino N (Thorn and Mikita, 1992).
459 Therefore, abiotic N retention could be much more prevalent in soil than assumed until now.

460 Microbial inoculation did neither reduce the abiotic N immobilization nor the composition of
461 immobilized N in this study (Table 3, Figure 2). High concentrations of NO_2^- are toxic to microbes
462 (Bollag and Henninger, 1978), the activities of microbes could be depressed due to the large applied
463 NO_2^-, which is very likely the reason why we observed no significant impact of microbial inoculation
464 on abiotic N immobilization.

4.4 Soil N and C interplay

Nitrogen is not only the essential element for biological C assimilation, but also acts as important N-joint to connect C moieties in SOM, implying that soil N and C sequestration interact with each other via biological and chemical processes (Cassman et al., 1998; Said-Pullicino et al., 2014; Knicker, 2011a). Heterocyclic C-N compounds represent the most recalcitrant C and N compounds in soil, whose residence time can be up to hundreds of years (López-Martín et al., 2017). Lignin dimers and aromatic compounds have good ability to incorporate N fertilizer into SON and reduce its availability (Reichel et al., 2018; Wei et al., 2020), the structure of immobilized N might be black and amide-N found in this study.

Comparing GOM and FOM, it was found that SOM rich in black N demonstrated relatively higher thermal stability, lower volatile matter proportion and total ion intensity, while SOM with lower black N content shew higher volatile matter proportion and total ion intensity, but lower thermal stability (Figure 5 and Table 4). However, it needs to be further tested that to how much extend the black N contributes to the thermal stability of SOM, as well as how the SOM thermal stability affects its bioavailability.

5. Conclusion

The abiotic NO_2^-–SOM reactions in this study led to a retention of approximately 6 % of nitrite-N added to forest, grassland, and agricultural soils, in which fulvic acid exhibited a much higher ability to immobilize NO_2^- than the humus as a whole. According to the solid-state CP-MAS ^{15}N-NMR analysis, chemically immobilized N in SOM existed mainly in the form of amides and pyrroles. And Py-FI mass spectroscopy revealed that forest humus, which was enriched in black N, contained more lignin dimers and aryl- and olefin-C and shew relatively higher thermal stability compared with grassland humus. Our results revealed that the role of chemical reactions in soil N retention cannot be neglected, since chemical N immobilization not only reduces the bioavailability of N, but also plays a significant role in soil C and N interplay.

Acknowledgement

This study was supported by Guangdong Major Project of Basic and Applied Basic Research (2020B0301030004), Guangdong Province Key Laboratory for Climate Change and Natural Disaster Studies (Grant 2020B1212060025), the German Federal Ministry of Education and Research (BMBF) in the framework of the BonaRes INPLAMINT project (grant no. 031B0508A), by Innovation Group Project of Southern Marine Science and Engineering Guangdong Laboratory (Zhuhai) (No. 311021009), and the Chinese Scholarship Council (scholarship no. 201406890023). The authors would like to thank José M. De la Rosa, Paloma Campos Díaz de Mayorga, Marina Concepcion Paneque Carmona, Marta Velasco Molina, and Anna Zelia Almeida de Franca e Miller for their kind support during the experiment.

References

Abe, T., Maie, N., Watanabe, A., 2005. Investigation of humic acid N with X-ray photoelectron spectroscopy: Effect of acid hydrolysis and comparison with N-15 cross polarization/magic angle spinning nuclear magnetic resonance spectroscopy. Org. Geochem. 36(11), 1490-1497.

Austin, A.T., 1961. Nitrosation in organic chemistry. Sci. Prog. XLIX, 619-640.

Azhar, E.S., Verhe, R., Proot, M., Sandra, P., Verstraete, W., 1989. Fixation of nitrite nitrogen during the humification of alpha-naphthol in soil suspensions. J. Agric. Food Chem. 37(1), 262-266.

Bollag, J.M., Henninger, N.M., 1978. Effects of nitrite toxicity on soil bacteria under aerobic and anaerobic conditions. Soil Biol. and Biochem. 10(5), 377-381.

Cassman, K.G., Peng, S., Olk, D.C., Ladha, J.K., Reichardt, W., Dobermann, A., Singh, U., 1998. Opportunities for increased nitrogen-use efficiency from improved resource management in irrigated rice systems. Field Crops Res. 56(1-2), 7-39.

Dail, D.B., Davidson, E.A., Chorover, J., 2001. Rapid abiotic transformation of nitrate in an acid forest soil. Biogeochemistry 54(2), 131-146.

Fitzhugh, R.D., Christenson, L.M., Lovett, G.M., 2003a. The Fate of $^{15}NO_2^-$ Tracer in Soils under Different Tree Species of the Catskill Mountains, New York. Soil Sci. Soc. Am. J. 67, 1257-1265.

Fitzhugh, R.D., Lovett, G.M., Venterea, R.T., 2003b. Biotic and abiotic immobilization of ammonium, nitrite, and nitrate in soils developed under different tree species in the Catskill Mountains, New York, USA. Global Change Biol. 9(11), 1591-1601.

Fontaine, S., Barot, S., Barre, P., Bdioui, N., Mary, B., Rumpel, C., 2007. Stability of organic carbon in deep soil layers controlled by fresh carbon supply. Nature 450(7167), 277-280.

Galloway, J.N., Townsend, A.R., Erisman, J.W., Bekunda, M., Cai, Z., Freney, J.R., Martinelli, L.A., Seitzinger, S.P., Sutton, M.A., 2008. Transformation of the nitrogen cycle: recent trends, questions, and potential solutions. Science 320(5878), 889-892.

Gillespie, A.W., Walley, F.L., Farrell, R.E., Leinweber, P., Schlichting, A., Eckhardt, K.U., Regier, T.Z., Blyth, R.I.R., 2009. Profiling rhizosphere chemistry: Evidence from carbon and nitrogen K-Edge XANES and pyrolysis-FIMS. Soil Sci. Soc. Am. J. 73(6), 2002-2012.

Gondar, D., Lopez, R., Fiol, S., Antelo, J.M., Arce, F., 2005. Characterization and acid–base properties of fulvic and humic acids isolated from two horizons of an ombrotrophic peat bog. Geoderma 126(3), 367-374.

Gruber, N., Galloway, J.N., 2008. An Earth-system perspective of the global nitrogen cycle. Nature 451(7176), 293-296.

Islam, A., Chen, D., White, R.E., Weatherley, A., 2008. Chemical decomposition and fixation of nitrite in acidic pasture soils and implications for measurement of nitrification. Soil Biol. & Biochem. 40(1), 262-265.

ISO, 2005. ISO 10390:2005 soil quality – determination of pH. International Organization for Standardization

539 Isobe, K., Koba, K., Suwa, Y., Ikutani, J., Kuroiwa, M., Fang, Y., Yoh, M., Mo, J., Otsuka, S., Senoo,
540 K., 2012. Nitrite transformations in an N-saturated forest soil. Soil Biol. & Biochem. 52, 61-63.

541 Kikugawa, K., Kato, T., 1988. Formation of a mutagenic diazoquinone by interaction of phenol with
542 nitrite. Food Chem. Toxicol. 26(3), 209-214.

543 Knicker, H., 2007. How does fire affect the nature and stability of soil organic nitrogen and carbon? A
544 review. Biogeochemistry 85(1), 91-118.

545 Knicker, H., 2011a. Soil organic N - An under-rated player for C sequestration in soils? Soil Biol. &
546 Biochem. 43(6), 1118-1129.

547 Knicker, H., 2011b. Solid state CPMAS ^{13}C and ^{15}N NMR spectroscopy in organic geochemistry and
548 how spin dynamics can either aggravate or improve spectra interpretation. Org. Geochem. 42(8),
549 867-890.

550 Leinweber, P., Jandl, G., Eckhardt, K.U., Schulten, H.R., Schlichting, A., Hofmann, D., 2009a.
551 Analytical pyrolysis and soft-ionization mass spectrometry, biophysico ‐ chemical processes
552 involving natural nonliving organic matter in environmental systems, pp. 539-588.

553 Leinweber, P., Kruse, J., Baum, C., Arcand, M.M., Knight, J.D., Farrell, R.E., Eckhardt, K.u., Kiersch,
554 K., Jandl, G., 2013. Advances in understanding organic nitrogen chemistry in soils using state-of-
555 the-art analytical techniques. Adv. Agron. 119, 83-151.

556 Leinweber, P., Walley, F., Kruse, J., Jandl, G., Eckhardt, K.U., Blyth, R.I.R., Regier, T., 2009b.
557 Cultivation affects soil organic nitrogen: Pyrolysis-mass spectrometry and nitrogen K-edge
558 XANES spectroscopy evidence. Soil Sci. Soc. Am. J. 73(1), 82-92.

559 Lewis, D.B., Kaye, J.P., 2012. Inorganic nitrogen immobilization in live and sterile soil of old-growth
560 conifer and hardwood forests: implications for ecosystem nitrogen retention. Biogeochemistry
561 111(1), 169-186.

562 López-Martín, M., Nowak, K.M., Milter, A., Knicker, H., 2017. Incorporation of N from burnt and
563 unburnt ^{15}N grass residues into the peptidic fraction of fire affected and unaffected soils. J. Soils
564 and Sediments 17(6), 1554-1564.

565 Nelson, D. W., 1967. Chemical transformations of nitrite in soils, Iowa State University. Ph.D: 150.

566 Reichel, R., Wei, J., Islam, M.S., Schmid, C., Wissel, H., Schroder, P., Schloter, M., Bruggemann, N.,
567 2018. Potential of wheat straw, spruce sawdust, and lignin as high organic carbon soil amendments
568 to improve agricultural nitrogen retention capacity: An incubation study. Frontiers Plant Sci. 9, 900.

569 Riordan, E., Minogue, N., Healy, D., O'Driscoll, P., Sodeau, J.R., 2005. Spectroscopic and optimization
570 modeling study of nitrous acid in aqueous solution. J. Phys. Chem. A 109(5), 779-786.

571 Rousseau, B., Rosazza, J.P.N., 1998. Reaction of ferulic acid with nitrite: Formation of 7-hydroxy-6-
572 methoxy-1,2(4H)-benzoxazin-4-one. J. Agr. Food Chem. 46(8), 3314-3317.

573 Said-Pullicino, D., Cucu, M.A., Sodano, M., Birk, J.J., Glaser, B., Celi, L., 2014. Nitrogen
574 immobilization in paddy soils as affected by redox conditions and rice straw incorporation.
575 Geoderma 228, 44-53.

Schmidt-Rohr, K., Mao, J.D., Olk, D.C., 2004. Nitrogen-bonded aromatics in soil organic matter and their implications for a yield decline in intensive rice cropping. Proc. Natl. Acad. Sci. U.S.A. 101(17), 6351-6354.

Schnitzer, M., Schulten, H.R., 1992. The analysis of soil organic matter by pyrolysis-field ionization mass spectrometry. Soil Sci. Soc. Am. J. 56(6), 1811-1817.

Stevenson, F.J., 1995. Humus Chemistry: Genesis, Composition, Reactions, Second Edition, 72. American Chemical Society.

Su, H., Cheng, Y., Oswald, R., Behrendt, T., Trebs, I., Meixner, F.X., Andreae, M.O., Cheng, P., Zhang, Y., xf, schl, U., 2011. Soil nitrite as a source of atmospheric HONO and OH radicals. Science 333(6049), 1616-1618.

Thorn, K.A., Arterburn, J.B., Mikita, M.A., 1992. Nitrogen-15 and carbon-13 NMR investigation of hydroxylamine-derivatized humic substances. Environ. Sci. & Technol. 26(1), 107-116.

Thorn, K.A., Cox, L.G., 2009. N-15 NMR spectra of naturally abundant nitrogen in soil and aquatic natural organic matter samples of the International Humic Substances Society. Org. Geochem. 40(4), 484-499.

Thorn, K.A., Cox, L.G., 2016. Nitrosation and nitration of fulvic acid, peat and coal with nitric acid. Plos One 11(5).

Thorn, K.A., Mikita, M.A., 1992. Humic substances ammonia fixation by humic substances: a nitrogen-15 and carbon-13 NMR study. Sci. Total Environ. 113(1), 67-87.

Thorn, K.A., Mikita, M.A., 2000. Nitrite fixation by humic substances: Nitrogen-15 nuclear magnetic resonance evidence for potential intermediates in chemodenitrification. Soil Sci. Soc. Am. J. 64(2), 568-582.

VanCleemput, O., Samater, A.H., 1996. Nitrite in soils: Accumulation and role in the formation of gaseous N compounds. Fertil. Res. 45(1), 81-89.

Venterea, R.T., 2007. Nitrite-driven nitrous oxide production under aerobic soil conditions: kinetics and biochemical controls. Global Change Biol. 13(8), 1798-1809.

Weber, J.H., Wilson, S.A., 1975. The isolation and characterization of fulvic acid and humic acid from river water. Water Res. 9(12), 1079-1084.

Wei, J., Amelung, W., Lehndorff, E., Schloter, M., Vereecken, H., Brüggemann, N., 2017. N_2O and NO_x emissions by reactions of nitrite with soil organic matter of a Norway spruce forest. Biogeochemistry 132(3), 325–342.

Wei, J., Ibraim, E., Brüggemann, N., Vereecken, H., Mohn, J., 2019. First real-time isotopic characterisation of N_2O from chemodenitrification. Geochim. Cosmochim. Acta 267, 17-32.

Wei, J., Reichel, R., Islam, M.S., Wissel, H., Amelung, W., Brüggemann, N., 2020. Chemical Composition of high organic carbon soil amendments affects fertilizer-derived N_2O emission and nitrogen immobilization in an oxic sandy loam. Front. Environ. Sci. 8, 15.

Zacharias, S., Bogena, H., Samaniego, L., Mauder, M., Fuß, R., Pütz, T., Frenzel, M., Schwank, M., Baessler, C., Butterbach-Bahl, K., Bens, O., Borg, E., Brauer, A., Dietrich, P., Hajnsek, I., Helle,

614 G., Kiese, R., Kunstmann, H., Klotz, S., Munch, J.C., Papen, H., Priesack, E., Schmid, H.P.,
615 Steinbrecher, R., Rosenbaum, U., Teutsch, G., Vereecken, H., 2011. A network of terrestrial
616 environmental observatories in Germany. Vadose Zone J. 10, 955-973.

617 Zaehle, S., 2013. Terrestrial nitrogen–carbon cycle interactions at the global scale. Philos. Trans. R. Soc.
618 Lond., B, Biol. Sci. 368(1621).

Table S1. Peak areas as percentage of total N for CP/MAS ^{15}N-NMR spectra.

Treatment	50–-50 ppm (nitro/oxime/NO_3^-, %)	-100–-180 ppm (nitrile, %)	-180–-230 ppm (pyrrole, %)	-230–-285 ppm (amide, %)	-285–-320 ppm (amino, %)
GOM	-	-	-	99	-
GOM+$^{15}NO_2^-$ (S) [a]	22	8	8	51	8
GOM+$^{15}NO_2^-$+M (S) [c]	26	6	7	51	8
GOM+$^{15}NO_2^-$+M (L) [b]	14	5	9	65	4
FOM	-	-	36	63	-
FOM+$^{15}NO_2^-$ (S) [d]	30	3	9	49	7
FOM+$^{15}NO_2^-$ (L) [e]	10	6	9	66	6

Note:

[a] Solid phase of NO_2^- amended grassland humus without microbes;

[b] Liquid phase of NO_2^- amended grassland humus with microbes;

[c] Solid phase of NO_2^- amended grassland humus with microbes;

[d] Solid phase of NO_2^- amended forest humus without microbes;

[e] Liquid phase of NO_2^- amended forest humus without microbes.

Table S2. Ion intensity of ^{15}N-NO_2^- amended forest humus extract.

m/z	Ion intensity (% total ion intensity)	
	FOM + $^{15}NO_2^-$	FOM + $^{15}NO_2^-$ + M
77	0.0931 ± 0.0122	0.1170 ± 0.0032
102	0.1188 ± 0.0165	0.0876 ± 0.0074
163	0.4623 ± 0.0359	**0.6268 ± 0.0638***
173	0.1126 ± 0.0010	0.1254 ± 0.0062
205	0.1444 ± 0.0058	**0.1273 ± 0.0039***
403	0.0702 ± 0.0069	**0.0883 ± 0.0084***
445	0.0402 ± 0.0029	0.0506 ± 0.0055
543	0.0139 ± 0.0016	0.0194 ± 0.0030
586	0.0148 ± 0.0022	0.0219 ± 0.0035
610	0.0158 ± 0.0012	**0.0125 ± 0.0005***
619	0.0086 ± 0.0010	0.0126 ± 0.0020
629	0.0073 ± 0.0019	**0.0118 ± 0.0012***
711	0.0028 ± 0.0001	0.0053 ± 0.0009*
719	0.0083 ± 0.0009	**0.0043 ± 0.0011****
755	0.0018 ± 0.0008	**0.0039 ± 0.0003***
779	0.0035 ± 0.0006	**0.0014 ± 0.0008***
827	0.0007 ± 0.0002	0.0021 ± 0.0006
880	0.0027 ± 0.0004	**0.0005 ± 0.0007***

Table S3. Ion intensity of ^{15}N-NO_2^- amended grassland humus extract.

m/z	Ion intensity (% total ion intensity)		m/z	Ion intensity (% total ion intensity)	
	GOM + $^{15}NO_2^-$	GOM + $^{15}NO_2^-$ + M		GOM + $^{15}NO_2^-$	GOM + $^{15}NO_2^-$ + M
48	0.017 ± 0.001	**0.013 ±0.001****	482	0.221 ± 0.002	**0.168 ±0.030***
78	0.063 ± 0.001	**0.069 ±0.002****	486	0.116 ± 0.007	**0.093 ±0.004****
79	0.079 ± 0.005	0.075 ±0.002	488	0.133 ± 0.003	**0.115 ±0.007****
84	0.301 ± 0.012	0.302 ±0.013	489	0.100 ± 0.006	**0.082 ±0.007***
94	0.107 ± 0.003	**0.114 ±0.001***	490	0.152 ± 0.007	**0.117 ±0.012****
101	0.103 ± 0.003	**0.115 ±0.003****	492	0.175 ± 0.008	**0.139 ±0.020***
114	0.112 ± 0.008	0.124 ±0.008	499	0.083 ± 0.002	**0.067 ±0.007***
115	0.113 ± 0.003	**0.149 ±0.011****	500	0.104 ± 0.002	**0.084 ±0.006****
115	0.113 ± 0.003	**0.149 ±0.011****	502	0.128 ± 0.003	**0.102 ±0.010****
120	0.094 ± 0.004	**0.105 ±0.003****	504	0.143 ± 0.006	**0.109 ±0.012****
126	0.226 ± 0.008	**0.263 ±0.019***	524	0.107 ± 0.006	**0.087 ±0.010***
127	0.170 ± 0.002	**0.204 ±0.012****	525	0.100 ± 0.006	**0.076 ±0.012***
128	0.118 ± 0.009	**0.133 ±0.004***	526	0.100 ± 0.008	**0.079 ±0.009***
129	0.149 ± 0.011	**0.174 ±0.009***	533	0.088 ± 0.006	**0.066 ±0.011***
130	0.072 ± 0.003	**0.089 ±0.009***	538	0.102 ± 0.007	**0.076 ±0.014***
137	0.082 ± 0.002	**0.093 ±0.006***	546	0.092 ± 0.010	**0.070 ±0.008***
138	0.116 ± 0.003	**0.157 ±0.013****	550	0.094 ± 0.008	**0.069 ±0.011***
139	0.103 ± 0.003	**0.129 ±0.008****	551	0.084 ± 0.008	**0.058 ±0.013***
140	0.153 ± 0.004	**0.181 ±0.004****	553	0.071 ± 0.004	**0.045 ±0.013***
143	0.097 ± 0.005	**0.122 ±0.011***	554	0.086 ± 0.006	**0.066 ±0.010***
144	0.088 ± 0.011	**0.114 ±0.011***	569	0.056 ± 0.004	**0.039 ±0.007***
145	0.112 ± 0.004	**0.147 ±0.009****	580	0.066 ± 0.009	**0.044 ±0.009***
148	0.123 ± 0.004	**0.146 ±0.005****	592	0.078 ± 0.007	**0.061 ±0.007***
150	0.140 ± 0.008	**0.168 ±0.012***	599	0.038 ± 0.001	**0.027 ±0.002****
156	0.094 ± 0.003	**0.107 ±0.003****	600	0.044 ± 0.004	**0.035 ±0.002***
162	0.151 ± 0.007	**0.174 ±0.013***	602	0.048 ± 0.005	**0.038 ±0.004 ***
163	0.271 ± 0.016	**0.334 ±0.035***	619	0.052 ± 0.007	**0.034 ±0.007***
164	0.123 ± 0.001	**0.158 ±0.022***	622	0.058 ± 0.009	**0.038 ±0.008***
168	0.136 ± 0.011	**0.179 ±0.017***	630	0.037 ± 0.003	**0.026 ±0.005***
171	0.084 ± 0.007	**0.101 ±0.004***	633	0.040 ± 0.004	**0.031 ±0.004***
183	0.139 ± 0.008	**0.163 ±0.011***	636	0.044 ± 0.003	**0.030 ±0.007***
185	0.106 ± 0.005	**0.123 ±0.007***	639	0.026 ± 0.002	**0.022 ±0.002***
186	0.114 ± 0.006	**0.150 ±0.020***	642	0.028 ± 0.002	**0.023 ±0.002***
188	0.101 ± 0.004	**0.116 ±0.007***	669	0.018 ± 0.002	**0.014 ±0.001***
205	0.103 ± 0.002	**0.120 ±0.008***	670	0.025 ± 0.002	**0.016 ±0.001****
215	0.081 ± 0.005	**0.106 ±0.014***	672	0.025 ± 0.003	**0.018 ±0.003***
216	0.109 ± 0.005	**0.138 ±0.016***	685	0.017 ± 0.003	**0.011 ±0.001***
228	0.190 ± 0.005	**0.250 ±0.007****	697	0.016 ± 0.001	**0.011 ±0.001****
229	0.122 ± 0.006	**0.160 ±0.018***	699	0.015 ± 0.001	**0.013 ±0.001***
242	0.423 ± 0.011	**0.574 ±0.019****	711	0.015 ± 0.001	**0.009 ±0.002****
243	0.246 ± 0.009	**0.292 ±0.017****	713	0.016 ± 0.002	**0.010 ±0.001****

256	1.372 ± 0.118	**1.942 ±0.125****	724	0.018 ± 0.001	**0.014 ±0.001***
269	0.209 ± 0.009	**0.269 ±0.028***	727	0.015 ± 0.001	**0.012 ±0.001***
270	0.495 ± 0.029	**0.655 ±0.043****	741	0.020 ± 0.001	**0.014 ±0.001****
271	0.292 ± 0.034	**0.369 ±0.027***	756	0.021 ± 0.002	**0.015 ±0.002***
284	0.739 ± 0.034	**0.927 ±0.071****	780	0.015 ± 0.002	**0.009 ±0.001***
297	0.257 ± 0.016	**0.322 ±0.034***	786	0.021 ± 0.003	**0.012 ±0.003***
298	0.338 ± 0.013	**0.449 ±0.028****	796	0.013 ± 0.002	**0.009 ±0.001***
312	0.418 ± 0.021	**0.512 ±0.044***	800	0.036 ± 0.009	**0.018 ±0.001***
313	0.285 ± 0.009	**0.325 ±0.019***	801	0.028 ± 0.002	**0.018 ±0.005***
326	0.216 ± 0.007	**0.275 ±0.032***	804	0.032 ± 0.003	**0.020 ±0.006***
327	0.175 ± 0.008	**0.202 ±0.012***	807	0.014 ± 0.001	**0.010 ±0.002***
354	0.371 ± 0.015	**0.411 ±0.006****	808	0.013 ± 0.002	**0.007 ±0.003***
394	0.273 ± 0.008	**0.316 ±0.026***	811	0.014 ± 0.003	**0.007 ±0.002***
398	0.342 ± 0.006	**0.307 ±0.017***	827	0.014 ± 0.003	**0.009 ±0.001***
442	0.210 ± 0.005	**0.196 ±0.000****	829	0.021 ± 0.003	**0.012 ±0.003***
445	0.105 ± 0.005	**0.091 ±0.003****	830	0.040 ± 0.006	**0.024 ±0.006***
446	0.158 ±0.002	**0.150 ±0.004***	831	0.032 ± 0.006	**0.020 ±0.004***
459	0.126 ± 0.002	**0.094 ±0.014****	840	0.013 ± 0.000	**0.009 ±0.001****
460	0.155 ± 0.003	**0.139 ±0.007***	864	0.009 ± 0.001	**0.006 ±0.002***
462	0.184 ± 0.004	**0.160 ±0.009****	871	0.017 ± 0.002	**0.011 ±0.001****
470	0.155 ± 0.005	**0.138 ±0.006***	875	0.012 ± 0.003	**0.006 ±0.001***
471	0.104 ± 0.002	**0.091 ±0.006***	881	0.009 ± 0.001	**0.005 ±0.001***
472	0.128 ± 0.006	**0.110 ±0.005****	886	0.014 ± 0.001	**0.009 ±0.002***
474	0.148 ± 0.008	**0.128 ±0.002****	896	0.008 ± 0.001	**0.005 ±0.001****
476	0.169 ± 0.003	**0.143 ±0.016***			